Pulse front tilt measurement of femtosecond laser pulses

Nikolay Dimitrov[a], Lyubomir Stoyanov[a], Ivan Stefanov[a],
Alexander Dreischuh[a,*], Peter Hansinger[b,c], Gerhard G. Paulus[b,c]

[a] *Department of Quantum Electronics, Faculty of Physics, Sofia University "St. Kliment Ohridski," 5, J. Bourchier Blvd., Sofia-1164, Bulgaria*
[b] *Institute for Optics and Quantum Electronics, Friedrich-Schiller-University, Max-Wien-Platz 1, D-07743 Jena, Germany*
[c] *Helmholtz Institute Jena, Helmholtzweg 4, D-07743 Jena, Germany*

Abstract

In this work we report experimental investigations of an intentionally introduced pulse front tilt on femtosecond laser pulses by using an inverted field correlator/interferometer. A reliable criterion for the precision in aligning (in principle) dispersionless systems for manipulating ultrashort pulses is developed, specifically including cases when the pulse front tilt is a result of a desired spatio-temporal coupling. The results obtained using two low-dispersion diffraction gratings are in good qualitative agreement with the data from a previously developed analytical model and from an independent interferometric measurement.

Keywords: Ultrafast measurements, femtosecond pulses, pulse front tilt, inverted field correlator, inverted field interferometer, (auto)correlation
PACS: 42.65.Re, 42.79.Hp, 42.60.Jf, 42.60.By

1. Introduction

The pulse front tilt (PFT) is a specific spatio-temporal distortion of (ultra)fast optical pulses - the pulse front is tilted with respect to the direction of beam/pulse propagation, while its phase front remains perpendicular to it. This effect and its measurement becomes interesting for the scientific community in relation with the generation of femtosecond laser pulses in the

*Corresponding author. Tel.: (+359 2) 8161 611; fax: (+359 2) 868 88 13.
Email address: ald@phys.uni-sofia.bg (Alexander Dreischuh)

mid-eighties. With the pioneering work of Bor and co-workers [1] as well as of Martinez [2], many of the basic properties and relations have been extensively studied in the late eighties-first half of the nineties. Most of them, well known nowadays, can be found in textbooks (see e.g. [3]). In some cases the PFT is useful. When the lifetime of an amplifying medium is shorter than the driving laser pulse, pump pulses with tilted pulse fronts offer the possibility to progressively deposit the pump energy along the gain medium at a speed equal to the transient speed of the amplified wave (see e.g.[4, 5, 6, 7, 8]). Another example is the efficient phase-matched terahertz radiation generated by optical rectification of femtosecond laser pulses [9, 10] down to near-single-cycle terahertz pulse durations [11, 12, 13, 14]. In high harmonic generation experiments, pulses with tilted fronts enable the production of sources emitting a collection of angularly well-separated light beams, each consisting of an isolated attosecond pulse [15]. However, when PFT is present, the duration of the pulse is short only in a limited region of space [16] and the effective pulse duration increases. The connection between pulse front distortions and duration of femtosecond pulses have been experimentally analyzed by several groups. The most notable and exhausting studies besides of [17] are [18, 19]. Tilting of the pulse front of picosecond pulses after traveling through a prism [20] or diffraction on a grating [21] is well known [16]. The PFT is one of the major issues in chirped pulse amplification systems [22, 23, 24], caused by misaligned pulse stretchers and/or compressors. PFT can also occur when femtosecond pulses are focused [25, 26] or passed through birefrigent crystals [27]. Even the overlapping of femtosecond pulses with PFT is not simple anymore [28].

Specific diagnostic techniques for detecting and measuring PFT are available: tilted pulse front autocorrelation [29, 30, 31], spectrally resolved interferometry [32], Grating-Eliminated No-nonsense Observation of Ultrashort Incident Laser Light E-fields (GRENOUILLE) [33], and Cross-correlation Frequency-Resolved Optical Gating (XFROG) [34]. Angular dispersion and/or pulse front tilt was measured by several other groups and methods, where these were used also for alignment of the stretcher/compressor system of e.g. CPA lasers [35, 36, 37, 38, 39]. The usual interferometric second-harmonic autocorrelators based on Michelson or Mach-Zehnder-type schemes are not able to detect PFT unless one of the beams/pulses is inverted in space [17, 29, 30, 31, 32, 40, 41, 42] or cross-correlation between a tilted and a non-tilted pulse is realized [41]. In such inverted-field (IF) correlators, the delay between the pulses also depends on the particular transverse coordi-

nate across the beam. Hence, the recorded autocorrelation trace contains information on the effective broadening of the ultrashort pulse due to the PFT [40, 42].

In this work we report experimental investigations of intentionally introduced pulse front tilts on femtosecond laser pulses by using inverted field correlator/interferometer and compare the results with the data from a previously developed analytical model [43].

2. Theoretical model

Let us describe a Gaussian pulse/beam in a co-moving coordinate system as propagating along the z-axis, parallel to the time axis t (Fig. 1). For convenience, let us normalize the transverse spatial coordinate x to the speed of light c. Hence, the unit of x/c is $[x/c] = 1\,\mathrm{fs}$ and we have the correspondence $1\,\mathrm{fs} \leftrightarrow 0.3\,\mu\mathrm{m}$ for a central wavelength $\lambda_0 = 808\,\mathrm{nm}$ of the pulse spectrum (i.e. for a carrier-wave frequency $\omega = 2.356\,\mathrm{fs}^{-1}$). In Fig. 1a we show the pulse/beam intensity envelope in case there is zero PFT. It has a time duration t_0 and beam width r_0 (at $1/e^2$ intensity level). If the front of this pulse is tilted at an angle F with respect to the phase front (Fig. 1b), it will keep propagating in the same direction, however it will be characterized not by the initial parameters (t_0, r_0) but by its effective parameters t_1, t_2, r_1. Here t_1 denotes the relatively weakly increased pulse duration in one particular transverse cross-section, whereas t_2 is its vastly enhanced effective width across its whole cross-section. The relatively weak narrowing of the width of the beam we denote by r_1.

As shown in [43], the PFT of a Gaussian pulse can be described by interpreting the field envelope of the pulse/beam as a rotated ellipse. In the non-perturbed case the field amplitude of the ultrashort pulse can be expressed in the form

$$\tilde{E}(x,t) = E_0 \exp(-x^2/r_0^2 - t^2/t_0^2) \exp(-i\omega t), \tag{1}$$

where $\tilde{E}(x,t,F,\tau_d)$ denotes the field amplitude in the presence of a PFT. Here τ_d is the eventual offset (delay) of the pulse envelope with respect to the origin of the time coordinate axis.

If one performs a standard interferometric autocorrelation measurement of a pulse with tilted pulse front, the recorded signal will depend on the effective time t_1, but there will be no direct indication for the presence of

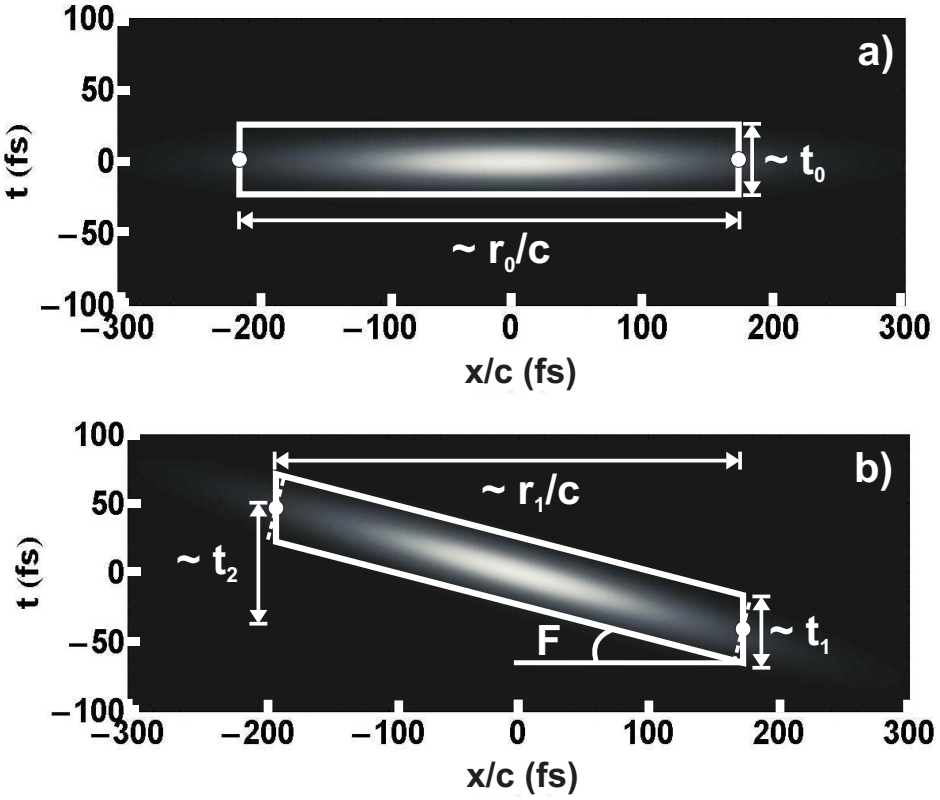

Figure 1: **a)** Intensity distribution of a Gaussian pulse/beam with a time duration t_0 and beam width r_0. **b)** Effective pulse/beam dimensions t_1, r_1, and t_2 of the same pulse/beam envelope rotated at a PFT angle F.

a PFT. The diagnostics and the evaluation of the PFT are possible with an IF interferometer/autocorrelator [41] as shown in Fig. 2. In essence, due to the double reflection of the beam in one of its arm and due to the single reflection in the another one, one of the beams is rotated by 180° with respect to the second one (around their common propagation axis). The normalized second-order autocorrelation signal obtained with Gaussian pulses with PFT in an IF autocorrelator has the form

$$B_2^F(F,\tau_d) = \frac{\int_{-\infty}^{+\infty}\int_{-\infty}^{+\infty} |\{\tilde{E}_1(x,t,F,\tau_d) + \tilde{E}_2(x,t,-F,0)\}^2|^2 dxdt}{2\int_{-\infty}^{+\infty}\int_{-\infty}^{+\infty} |\tilde{E}_i^2(x,t,F,\tau_d)|^2 dxdt}, \qquad (2)$$

where F is the PFT angle and the delay between the pulses τ_d is the

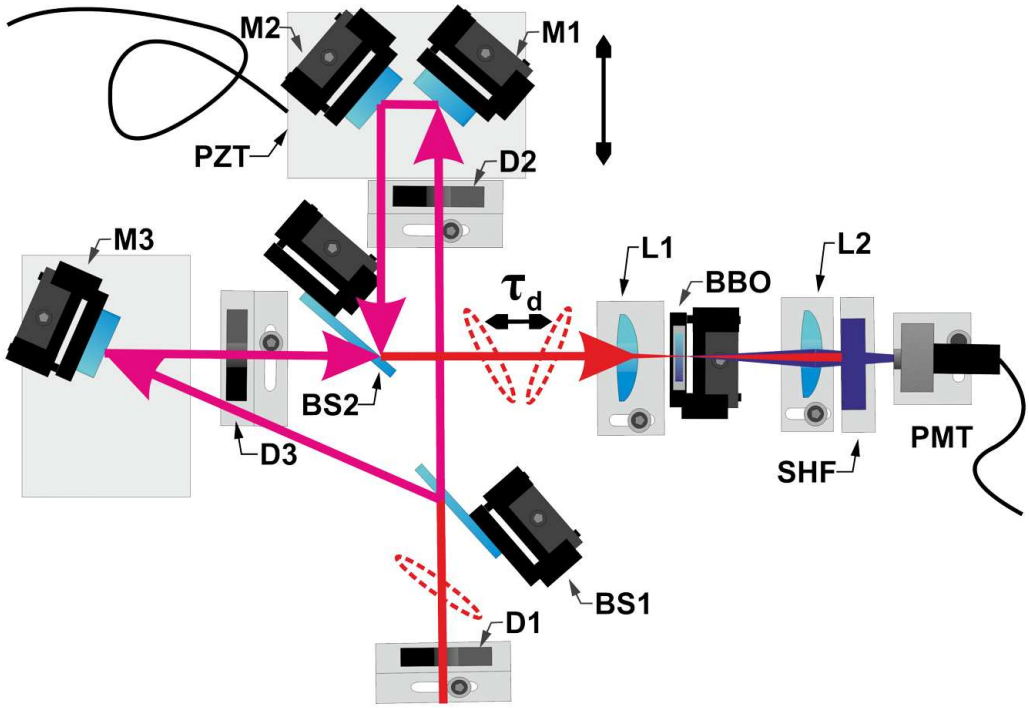

Figure 2: Autocorrelator sensitive to PFT for acquiring second-order interferometric autocorrelation. M1...M3 - protected silver flat mirrors, BS1, BS2 - beamsplitters ($45°/800nm$), D1, D2 - iris diaphragms, L1, L2 - lenses ($f = 3.5cm$), PMT - photomultiplier, PZT - piezotransducer-driven translation table, BBO - 50-μm thick crystal for second harmonic generation, SHF - filter transmitting the second harmonic. Ellipses (dashed contours) - pulses/beams with their respective PFTs.

temporal offset between the centers of the pulses measured at the propagation axis (see Fig. 2). The subscript $i = 1$ or 2 denotes one of the fields (irrespective which one, provided the first harmonic signals are equal in power/intensity after the second beamsplitter). Following the procedure described in [43], we obtain an analytic expression for the second-order autocorrelation signal in the presence of a PFT:

$$B_2^F(F, \tau_d) = AC_a + AC_b \cos(\omega\tau_d) + AC_c \cos(2\omega\tau_d), \tag{3}$$

where ω is the central frequency for the pulse spectrum and

$$\begin{aligned} AC_a &= 1 + 4r_0t_0 \exp(-2\tau_d^2/K^2)/(KL) \\ AC_b &= (16r_0t_0\sqrt{2/M} \exp[-2\tau_d^2(M - 8r_0^2t_0^2)/(K^2M)]) \\ AC_c &= 2r_0t_0 \exp(-2\tau_d^2/K^2)/(KL). \end{aligned} \tag{4}$$

The abbreviations K, L, and M are given by

$$\begin{aligned} K &= [r_0^2 + t_0^2 + (t_0^2 - r_0^2)\cos(2F)]^{1/2} \\ L &= [r_0^2 + t_0^2 + (r_0^2 - t_0^2)\cos(2F)]^{1/2} \\ M &= 3r_0^4 + 26r_0^2t_0^2 + 3t_0^4 - 3(r_0^2 - t_0^2)^2\cos(4F). \end{aligned} \tag{5}$$

This representation of the second-order autocorrelation function in three terms oscillating at frequencies 0, ω, and 2ω corresponds to the one adopted in the literature [3]. Physical intuition leads to the following suppositions for the influence of the PFT on the signal from an IF autocorrelator:

2.1. Lengthening of the autocorrelation

If the pulses in an IF autocorrelator have tilted fronts, one can expect that the time necessary for a complete passage of one of the pulses through the other should increase with increasing the PFT angle F. This should result in a lengthening of the autocorrelation curve and will reflect the effective lengthening of the pulses from t_0 (which is equal to t_1 for $F = 0$, i.e. for no PFT, but different from t_1 when a PFT is present) to an effective pulse length $t_2(F)$ (see Fig. 1). This $t_2(F)$ is the measured pulse duration in an IF autocorrelator.

2.2. Changes in fringe contrast

For the same reason (the inversion of the field in one of the arms of the correlator) the pulses never overlap completely across their space-time cross-sections except for PFT angles equal to zero and $\pi/2$. In a balanced correlator this will result in a reduction of the peak-to-background signal ratio from 8:1 to lower values for PFT angles F in the interval $(0, \pi/4)$. This situation is to be expected for ultrashort pulses, for which the space-time intensity ellipse has high ellipticity. For $F = \pi/4$, the two main axes of the space-time ellipses of the pulse/beam envelopes cross at an angle $2F = \pi/2$ and, because of their minimal overlap, the contrast is expected to be minimal. In the rather exotic limiting case of $F = \pi/2$, the intensity envelopes are rotated in such a way that r_0 is their *effective* time duration, whereas their *effective* spatial extent is t_0. This should not be interpreted as space-time inversion, but as an extreme rotation of the pulse fronts. The spatial and temporal axes x and t remain fixed and define the coordinate system for all transformations we perform.

The analytical model (Eqs. 3,4) predicts exactly the same behavior of the correlation signal. In Fig. 3 we demonstrate this by simulations for a pulse/beam with $t_0 = 25\,\mathrm{fs}$ and $r_0 = 65\,\mu\mathrm{m} \leftrightarrow 217\,\mathrm{fs}$.

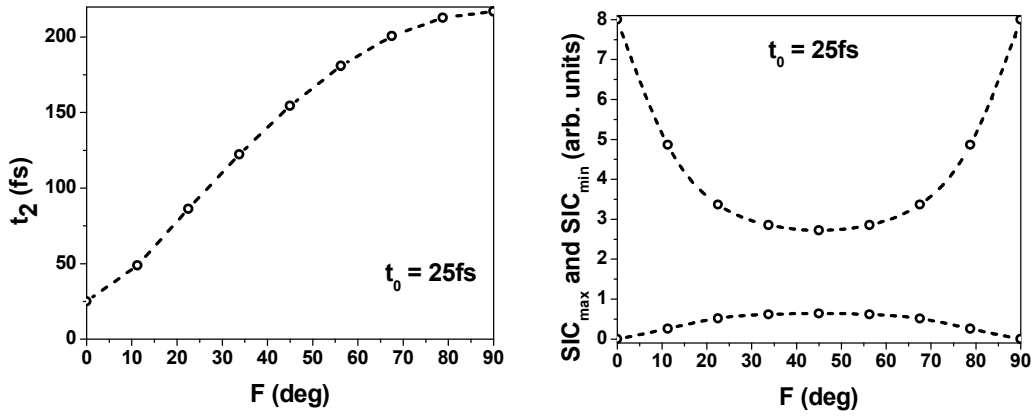

Figure 3: Effect of the PFT at an angle F on the simulated interferometric correlation (SIC) signal broadening of the effective pulse width t_2 (left) and change in the ratio between maximal (upper curve) and minimal signal (lower curve) SIC signal.

In the presence of a linear frequency modulation with a chirp-parameter a [3], the field amplitude of the ultrashort pulse without PFT can be written in the form

$$\tilde{E}(x,t,a) = E_0 \exp[-x^2/r_0^2 - (1-ia)t^2/t_0^2] \exp(-i\omega t). \tag{6}$$

Unfortunately we could not find an exact analytic solution for the signal of the second-order interferometric correlation $B_2^F(F,\tau_d,a)$ with non-zero PFT, but we solved the integral in Eq. 2 numerically. The results show that the two parameters important in this work – the change in the maximal and minimal signal of the simulated interferometric correlation (SIC) signal (and their ratio) – do not depend on the linear chirp (i.e. on the quadratic phase modulation) even for rather high values of the chirp-parameter (Fig. 4). An in-depth discussion on the changes in the correlation curves due to the linear chirp are outside the scope of this work but are well known.

This results allows to neglect the influence of the linear chirp in the further discussion and to assume that the width and the contrast of the correlation signal from an IF correlator depend solely on the PFT.

3. Experimental verification of the model

In this experiment we used pulses emitted from a commercial femtosecond oscillator (Ti-Light, Quantronix). Outside the cavity the pulses were extra compressed by 12 reflections on a cascade of chirped mirrors. These pulses

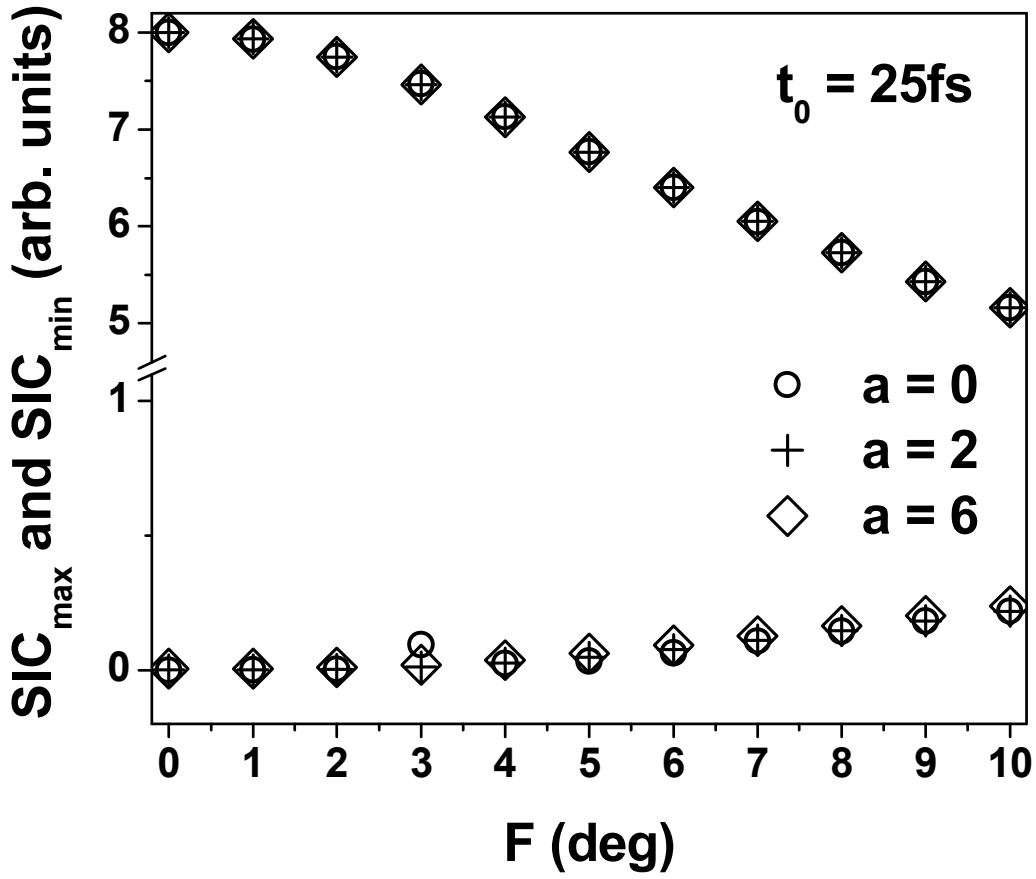

Figure 4: Influence of the quadratic phase modulation on the maximal and minimal signals of the simulated interferometric correlation for different values of the chirp-parameter a.

are free of PFT and have a duration $t_{\mathrm{FWHM}} = 29\,\mathrm{fs}$ ($t_0 = 25\,\mathrm{fs}$ at $1/e^2$ intensity-level). The central wavelength of the spectrum is $\lambda_0 = 808\,\mathrm{nm}$, the pulse repetition rate – some 80 MHz, the mean power of the emission typically 160 mW. In order to intentionally introduce PFT in the pulses we used diffraction gratings (see Fig. 5). By means of the flat mirror M5 the pulses are first redirected to the grating. The beam diffracted in first order is sent back on the preliminary fixed propagation path by the second flat mirror and M6 passing through three diaphragms (D4, D5, D1). This propagation axis is fixed after precise alignment of the correlator. The two flat mirrors M5 and M6 are mounted on a translation stage. They can be easily removed from the propagation path thus allowing switching from non-zero to zero PFT

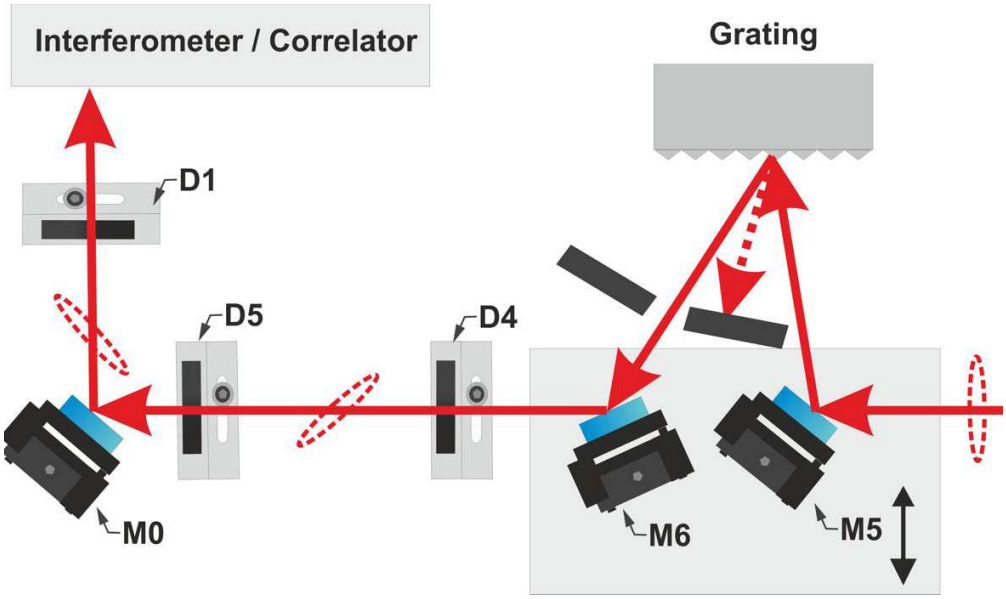

Figure 5: Setup for tilting the pulse fronts of femtosecond pulses by using reflective diffraction grating. Mx - flat protected silver mirrors, Dx - diaphragms, dashed ellipces - spatio-temporal orientation of the beam/pulse.

and vice versa. In this experiment we used two low-period binary reflective gratings G1 with 33 lines/mm and G2 with 160 lines/mm.

The home-built IF interferometer (Fig. 2) includes three flat silver mirrors (M1, M2, M3), a pair of beamsplitters (800 nm/45°), two iris diaphragms (D1, D2), lenses L1 and L2 with focal lengths $f = 3.5$ cm, a 50 μm thick Beta Barium Borate (BBO) crystal for second harmonic (SH) generation, and a filter SHF transmitting the SH signal. The variable delay between the pulses in the arms of the correlator is controlled by a piezo-driven translation stage PZT ($nanoX_{200SG}$, Piezosystem Jena) with 200 μm range of motion, power supply ENV 40 (Piezosystem Jena). The latter is driven by a voltage pulse generator (GW-Instek AGF 2124) and its output is monitored on an oscilloscope (Tektronix TDS 2012B). The SH signal is acquired by a photomultiplier PMT (Hamamatsu) and a computer equipped with LabView-controlled interface (National Instruments). When necessary, the beam size is measured with a charge-coupled device camera (Ophihr SP620U, format 1/1.8", pixel size 4.4 μm $\times$ 4.4 μm).

In order to be able to calculate the SIC signal $B_2^F(F, \tau_d)$ (Eq. 3) and to

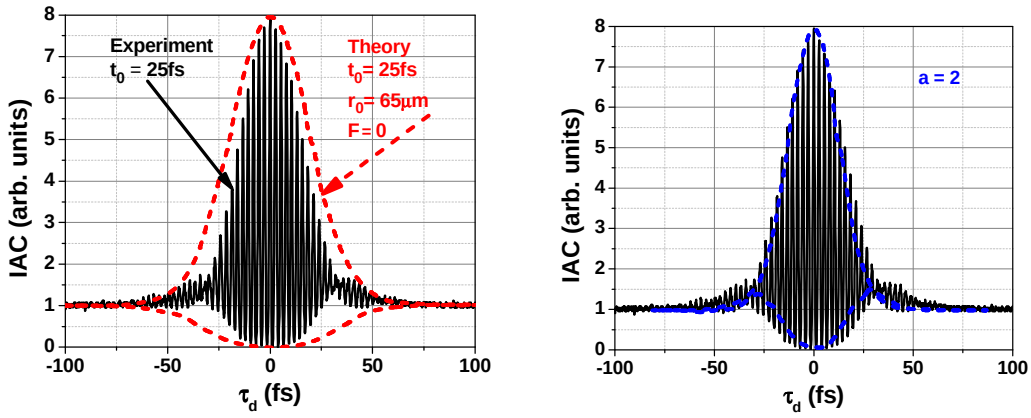

Figure 6: Comparison between the recorded interferometric autocorrelation signal (IAC) and the envelope of the numerically simulated IAC $B_2^F(F=0,\tau_d,a)$ (dashed curves). Left - chirp-parameter $a=0$, right - $a=2$.

compare it with the measured one with the IF autocorrelator, we need to know the three characteristics of the pulses with PFT - t_0, r_0, and F (see Fig. 1). As it will be seen later, the measurement of these three quantities is only seemingly trivial.

3.1. The model without PFT

As a first step we measured pulses with no PFT using the IF autocorrelator. The dimensions of the beam were measured at the front facet of the BBO crystal. In this way we obtained $t_0 = 25\,\mathrm{fs}$ and $r_0 = 65\,\mu\mathrm{m} \leftrightarrow 217\,\mathrm{fs}$ and substituted these values in our analytical model (Eqs. 3,4) keeping the PFT angle $F = 0$. The results are shown in Fig. 6. One can clearly recognize the phase modulation of the pulse. Although the statement that the chirp parameter has no influence on the maximal and minimal value of the signal of the interferometric correlation (see Fig. 4) is well-proven, we performed a test at the linear chirp parameter $a = 2$ (see right graph in Fig. 6).

It should be noted that the correlator used is an IF correlator; nevertheless at zero PFT this measurement is essentially the same as the usual autocorrelation measurement. We even do not need to determine r_0 since its value does not influence the interferometric autocorrelation (IAC). On the other hand, this measurement is necessary in order to check the alignment of the IF correlator. The result ($t_{\mathrm{FWHM}} = 29\,\mathrm{fs}$) is practically the same as the pulse duration obtained with a commercial FROG-device (GRENOUILLE, Swamp Optics), $t_{\mathrm{FWHM}} = 30\,\mathrm{fs}$. (It is worth mentioning that we failed to verify the

measured values for the pulse-front tilt angle by a GRENOUILLE-device because of the low pulse mean power due to the low diffraction efficiency of the used gratings.)

3.2. The model when PFT is present

In this case we need the three parameters t_0, r_0, and F (see Fig. 1) which requires more efforts. We used the following approach.

Using the IF correlator (Fig. 2), we could measure the pulse time duration t_2. Replacing the BBO crystal by a CCD-camera at the same location and using the same correlator with one arm blocked, we could measure the beam size r_1 in the presence of PFT at the front facet of the crystal (Fig. 7 left).

From the two measured quantities (r_1, t_2) we obtained

$$\begin{array}{rcl} r_0 & = & [(t_2 c)^2 + r_1^2]^{1/2}, \\ F & = & \arccos(r_1/r_0). \end{array} \tag{7}$$

In order to evaluate the correlation curve from the model Eq. 3, which describes the real situation in an IF correlator, and in order to compare it with the measured one, we also need the time duration t_0 of the pulse where no PFT lengthens the pulse due to the presence of the diffraction grating. One can measure t_0 by using e.g. a standard Michelson autocorrelator with no sensitivity against PFT (see Fig. 7 right). In this way, we got the (local) pulse duration t_1,

$$t_0 = t_1 \cos(F) = t_1 r_1 / \sqrt{(t_2 c)^2 + r_1^2}. \tag{8}$$

Following this procedure, i.e. using the described two configurations of the correlator and a CCD-camera in an interferometer with one blocked arm, we get the values of t_1, t_2, and r_1 and thus have all necessary input data for the algorithm for obtaining t_0, r_0, and F. The next step is to model the SIC signal for pulses with PFT.

4. Experimental results

4.1. Grating G1 (33 lines/mm)

We start by noting that the angular dispersion of a dispersive element (if present) leads to both PFT and pulse broadening, i.e. $t_0 = t_0(F)$. In case such a dispersive element is absent, $t_0(F = 0) =: T_0$. Using the IF

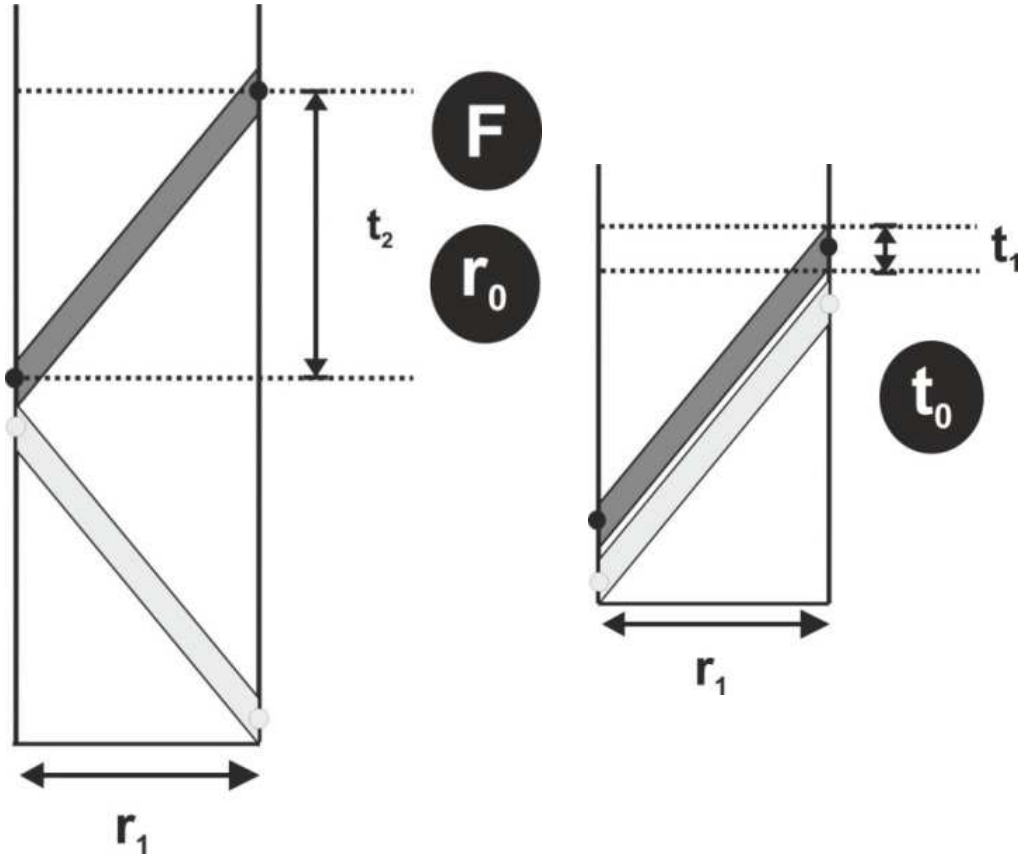

Figure 7: Schematic representation of the pulses/beams in an IF correlator/interferometer (left) and in a standard autocorrelator/interferometer with no PFT sensitivity (right). The measurable quantities are (t_2, r_1) - left, and (t_1, r_1)-right. The three parameters of interest (t_0, r_0, F) we are searching for are in black circles.

correlator (Fig. 2) we measured a pulse duration $T_0 = 25\,\mathrm{fs}$ (Fig. 5). Next we let the pulses pass through the setup for PFT induction by diffraction on the low-dispersion binary diffraction grating G1. Using the PFT-insensitive autocorrelator, we measured the pulse duration t_1. In this way we obtained $t_1 = 25\,\mathrm{fs}$, i.e. within the experimental accuracy $t_1 = T_0$. In other words, the low dispersion grating G1 does not cause noticeable pulse lengthening such that the real pulse duration after the PFT system should be $t_0 = 25\,\mathrm{fs}$ (since $T_0 \leq t_0(F) \leq t_1$; see Fig. 1a).

The transition from the PFT-insensitive (e.g. Michelson) autocorrelator with four mirrors (two times two in each arm) to an IF correlator was done

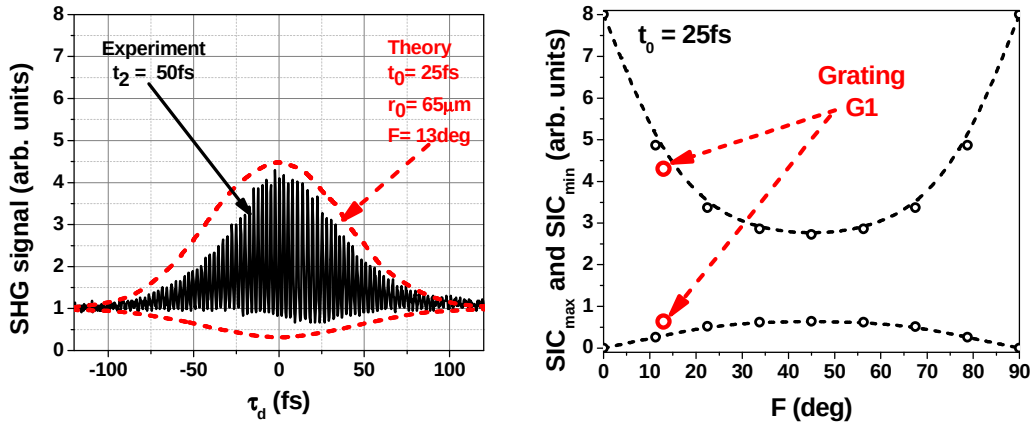

Figure 8: **Left**: Comparison between the experimentally measured interferometric correlation (IC) and the envelope of the simulated IC $B_2^F(F,\tau_d)$. **Right**: Position of the maximum and of the minimum of the experimentally obtained IC on the theoretically predicted curves (cf. Fig. 3).

by removing one of the mirrors and by tilting the remaining mirror (M3) and the beamsplitter (BS1, see Fig. 2). The alignment of the other arm remains unchanged. The beam passing through this unchanged arm serves as a reference beam for the optimal alignment of the other arm and warrants close similarity in the alignment of the two types of correlators. In this way we measured a correlation indicating a pulse width $t_2 = 50\,\mathrm{fs}$ (see Fig. 1b and Fig. 7 left). Here the presence of the PFT is clearly visible. As described above, the beam size $r_1 = 63\,\mu\mathrm{m}$ was measured by a CCD-camera. From the data for r_1 and t_2 we got $F = 13°$, $r_0 = 65\,\mu\mathrm{m} \leftrightarrow 217\,\mathrm{fs}$, $t_0 = 25\,\mathrm{fs}$.

At this point we already have all the necessary data r_0, t_0, and F for calculating the correlation signal $B_2^F(F,\tau_d)$ (Eqs. 3,4). In Fig. 8 (left) we show a comparison between the correlation signal of pulses with PFT measured with the IF correlator and the SIC signal $B_2^F(F,\tau_d)$. In the same figure (right panel) we mark the position of this experimental result on the theoretically predicted dependence.

As seen in Fig. 8, the comparison between the experimental and the theoretical results is qualitatively good. From the perfect 8 arbitrary units of the peak of the IC signal at zero delay τ_d when there is no PFT present, the signal decreases to 4.5 arbitrary units according to theory. This is close to the experimentally measured 4.3 relative units. For the minimum IC signal, which at no PFT should be zero, but now, because of the PFT, is expected to be 0.3, we measured an experimental value of 0.6 relative units.

4.2. Grating G2 (160 lines/mm)

The same measurements were repeated with the second diffraction grating G2. The first step was again to make use of the PFT-insensitive autocorrelator. Prior to the generation of the PFT we measured the duration of the untilted pulse to be $T_0 := t_0(F = 0) = 30\,\text{fs}$. After redirecting the input pulse/beam to G2, the shape of the correlation and the beam itself changed drastically. Even with the classical Michelson autocorrelator we measured a large increase in the pulse duration, $t_1 = 120\,\text{fs}$. This pulse lengthening is to be attributed, at least partially, to the time dispersion introduced by the diffraction grating [6]. Following the analysis in [3] (Eq. 1.120-1.123), accounting for the group-velocity dispersion ([3], Eq. 2.76) at a distance $L = 1.7\,\text{m}$ from the diffraction grating G2 to the BBO crystal and for the geometrical 10.8 times demagnification [41] in the correlator, we estimated an effective pulse broadening of the initial 30-fs pulses with a chirp parameter $a = 2$ up to 109 fs approaching the measured value of $t_1 = 120\,\text{fs}$.

In the IF correlator the registered pulse lengthening was huge and the scan range of the piezo-driven delay line was not enough to record the complete interferometric correlation curve. That is why we recorded only a bit more that half of it. Keeping in mind that the second-order correlation curve should be symmetric, this measurement should be significant, too. In this way we measured an effective pulse length $t_2 = 660\,\text{fs}$ of the pulses with PFT. By using the CCD-camera we measured the beam spot size to be $r_1 = 130\,\mu\text{m} \leftrightarrow 433\,\text{fs}$ at the front facet of the BBO crystal. Using the data for t_1, t_2, and r_1 we estimated $F = 57°$, $r_0 = 237\,\mu\text{m} \leftrightarrow 790\,\text{fs}$, and $t_0 = 66\,\text{fs}$. The large difference between the width of the pulse with no PFT ($T_0 = t_0(F = 0) = 30\,\text{fs}$) and the width of the pulse with PFT measured with the PFT-insensitive correlator ($t_0(F = 57deg) = 66\,\text{fs}$) is obvious. As mentioned, this pulse lengthening is to be attributed, at least partially, to the time dispersion introduced by the diffraction grating [6]. Using the obtained values for t_0, r_0, and F we calculated the correlation signal $B_2^F(F, \tau_d)$ from the IF autocorrelator. In Fig. 9 (left) we show again a comparison between the envelope of the theoretical curve and the result from the experiment.

As seen in Fig. 9, the comparison between the experimental and the theoretical results is again qualitatively good. From the perfect 8 arbitrary units of the peak of the IC signal at zero delay τ_d and with no PFT present, the signal theoretically decreases to 2.4 arbitrary units, which is close to the experimentally measured 2.1 relative units. For the minimum of the IC signal, which at no PFT should be zero, now, because of the PFT, we got

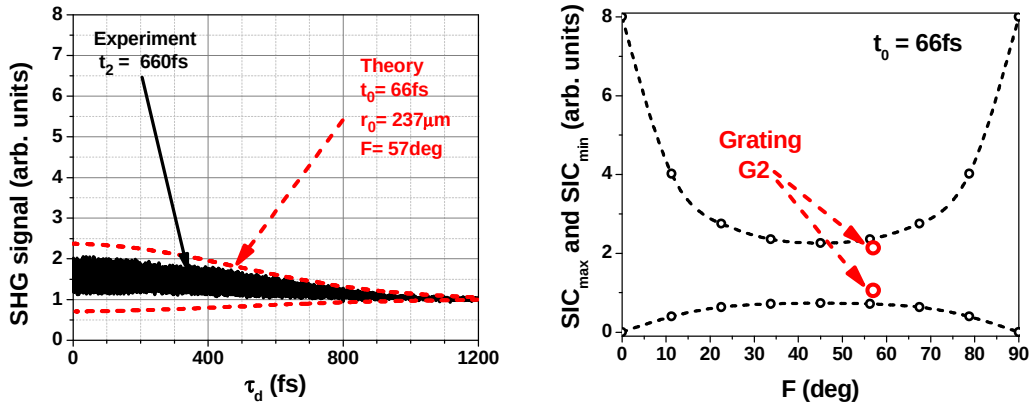

Figure 9: **Left**: Comparison between the measured interferometric correlation (IC) and the envelope of the calculated IC $B_2^F(F,\tau_d)$) by using the necessary parameters obtained experimentally. **Right**: Location of the maximum and of the minimum of the experimentally obtained IC on the theoretically predicted from $B_2^F(F,\tau_d)$ dependence of the minimum and the maximum of the SIC vs. PFT angle F.

theoretical value of 0.7 and measured an experimental value of 1.1 relative units.

In all measurements done with an interferometer and with a correlator, special attention was paid to the balance (equalization) of the mean powers of the beams in both arms of the setups. In this way we tried to eliminate the possibility that the visibility of the interference pattern at the entrance of the SHG crystal at a fixed delay becomes diminished due to the different mean powers of the beams. It should be noticed, however, that even in the presence of this effect the width of the correlation curves should not change due to it. In the measured signal we observed the two effects of the non-zero PFT predicted from physical reasons and used in formulating the theoretical model:
i) decrease of the peak-to-minimum IC signal ratio;
ii) lengthening of the IC signal due to the enhanced effective length of the pulse/beam with PFT.

We note that one can separately evaluate the PFT at the entrance of the BBO crystal once the PFT for the beam has been obtained using an independent interferometric technique for measuring the relation between beam width and PFT [46]. In essence, using an inverted field interferometer we measured the shift of the interference line of maximum contrast inside the beam vs. additional beam/pulse propagation path length causing this

shift. The slope of this dependence is indicative for the PFT angle F. These results are presented in [46]. In Table 1, we compare them with the ones obtained from the described experiments. Again it is fair to say that the comparison between these values is qualitatively good. Here it is worth also mentioning that the tilt of a pulse front also depends on whether the waves are plane waves or spherical ones. For the latter, the distances between the pulse front tilt element, the beam waist, and the measurement point need to be precisely taken into account (see e.g. [2, 44, 45]). Most probably this is one of the reasons why pulse front tilt values are slightly different (Table 1).

Table 1: Comparison between the values for the PFT angle F obtained interferometrically and as explained in the text for the two gratings G1 and G2. The beam size is taken at the position of the entrance facet of the BBO crystal in the IF correlator.

	Grating G1	Grating G2
Beam size at the BBO crystal	$63\,\mu$m	$130\,\mu$m
PFT angle F obtained interferometrically [46]	17°	58°
PFT angle F obtained in this work	13°	57°

5. Conclusion

The described experiments and their results confirm that the developed theoretical model [43] for the correlation signal from an inverted-field second-order correlator measuring incoming ultrashort pulses with pulse-front tilt is sound and its results are in a qualitative agreement with the experimental data. The decrease of the peak interferometric correlation signal and the increase of its minimal value from the zero level at precisely overlapped pulses along with the calibration curves in Fig. 3 (right) provide an easy to use method for aligning (in principle) dispersionless systems for manipulating ultrashort pulses, as well as in cases when the pulse front tilt is a result of a desired spatio-temporal coupling. Further experiments should be focused on confirming the quantitative correspondence and on evaluating possible limitations in the applicability of this method.

6. Acknowledgments

We acknowledge funding of the DFG within the framework of project PA 730/4-2 "New experimental approaches for unresolved problems of strong-field laser physics" and of the National Science Fund (Bulgaria) within the framework of project No. DFNI-T02/10.

7. Captions for the figures

Fig.1 – **a)** Intensity distribution of a Gaussian pulse/beam with a time duration t_0 and beam width r_0. **b)** Effective pulse/beam dimensions t_1, r_1, and t_2 of the same pulse/beam envelope rotated at a PFT angle F.

Fig.2 – Autocorrelator sensitive to PFT for acquiring second-order interferometric autocorrelation. M1...M3 - protected silver flat mirrors, BS1, BS2 - beamsplitters ($45°/800nm$), D1, D2 - iris diaphragms, L1, L2 - lenses ($f = 3.5cm$), PMT – photomultiplier, PZT - piezotransducer-driven translation table, BBO - 50-μm thick crystal for second harmonic generation, SHF - filter transmitting the second harmonic. Ellipses (dashed contours) - pulses/beams with their respective PFTs.

Fig.3 – Effect of the PFT at an angle F on the simulated interferometric correlation (SIC) signal broadening of the effective pulse width t_2 (left) and change in the ratio between maximal (upper curve) and minimal signal (lower curve) SIC signal.

Fig.4 – Influence of the quadratic phase modulation on the maximal and minimal signals of the simulated interferometric correlation for different values of the chirp-parameter a.

Fig.5 – Setup for tilting the pulse fronts of femtosecond pulses by using reflective diffraction grating. Mx - flat protected silver mirrors, Dx - diaphragms, dashed ellipces - spatio-temporal orientation of the beam/pulse.

Fig.6 – Comparison between the recorded interferometric autocorrelation signal (IAC) and the envelope of the numerically simulated IAC $B_2^F(F = 0, \tau_d, a)$ (dashed curves). Left - chirp-parameter $a = 0$, right - $a = 2$.

Fig.7 – Schematic representation of the pulses/beams in an IF correlator/interferometer (left) and in a standard autocorrelator/interferometer with no PFT sensitivity (right). The measurable quantities are (t_2, r_1) - left, and (t_1, r_1)-right. The three parameters of interest (t_0, r_0, F) we are searching for are in black circles.

Fig.8 – **Left**: Comparison between the experimentally measured interferometric correlation (IC) and the envelope of the simulated IC $B_2^F(F, \tau_d)$. **Right**: Position of the maximum and of the minimum of the experimentally obtained IC on the theoretically predicted curves (cf. Fig. 3).

Fig.9 – **Left**: Comparison between the measured interferometric correlation (IC) and the envelope of the calculated IC $B_2^F(F, \tau_d)$) by using the necessary parameters obtained experimentally. **Right**: Location of the maximum and of the minimum of the experimentally obtained IC on the theoretically predicted from $B_2^F(F, \tau_d)$ dependence of the minimum and the maximum of the SIC vs. PFT angle F.

8. Captions for the tables

Table 1 – Comparison between the values for the PFT angle F obtained interferometrically and as explained in the text for the two gratings G1 and G2. The beam size is taken at the position of the entrance facet of the BBO crystal in the IF correlator.

References

[1] Z. Bor, Z. Gogolak, and G. Szabo, "Femtosecond-resolution pulse-front distortion measurement by time-of-flight interferometry," Opt. Lett. **14**, 862–864 (1989).

[2] O. E. Martinez, "Grating and prism compressors in the case of finite beam size," J. Opt. Soc. Am. B **3**, 929–934 (1986).

[3] J.-C. Diels and W. Rudolph, Ultrashort Laser Pulse Phenomena, 2nd edition (Academic Press, Boston, 2006).

[4] H. Polland, T. Elsaesser, A. Seilmeier, W. Kaiser, M. Kussler, N. J. Marx, B. Sens, and K. H. Drexhage, "Picosecond dye laser emission in the infrared between 1.4 and 1.8μm," Appl. Phys. B **32**, 53–57 (1983).

[5] C. P. J. Barty, D. A. King, G. Y. Yin, K. H. Hahn, J. E. Field, J. F. Young, and S. E. Harris, "$12.8 - eV$ laser in neutral cesium," Phys. Rev. Lett. **61**, 2201-2204 (1988).

[6] S. Szatmari, G. Kuhnle, and P. Simon, "Pulse compression and traveling wave excitation scheme using a single dispersive element," Appl. Optics **29**, 5372–5379 (1990).

[7] J. C. Moreno, J. Nielsen, and L. B. Da Silva, "Traveling wave excitatioon and amplification in neon-like germanium $3p - 3s$ transitions," Opt. Commun. **110**, 585–589 (1994).

[8] J.-C. Chanteloup, E. Salmon, Ch. Sauteret, A. Migus, P. Zeitoun, A. Klisnick, A. Carillon, S. Hubert, D. Ros, P. Nickles, and M. Kalachnikov, "Pulse-front control of 15-TW pulses with tilted compressor, and application to the subpicosecond traveling-wave pumping of soft-x-ray laser," J. Opt. Soc. Am. B. **17**, 151–157 (2000).

[9] J. Hebling, G. Almasi, I. Z. Kozma, and J. Kuhl, "Velocity matching by pulse front tilting for large-area THz-pulse generation," Optics Express **10**, 1161–1166 (2002).

[10] J. A. Fülöp, L. Pálfalvi, G. Almási, J. Hebling, "Tilted-pulse-front pumping for phase matching and synchronization," Proc. SPIE **7501**, art. No. 75010D (2009).

[11] K.-L. Yeh, M. C. Hoffmann, J. Hebling, and K. A. Nelson, "Generation of $10\mu J$ ultrashort terahertz pulses by optical rectification," Appl. Phys. Lett. **171121**, art. No. 171121 (2007).

[12] A. G. Stepanov, L. Bonacina, S. V. Chekalin, and J.-P. Wolf, "Generation of $30\mu J$ single-cycle terahertz pulses at $100Hz$ repetition rate by optical rectification," Opt. Lett. **33**, 2497–2499 (2008).

[13] H. Hirori, A. Doi, F. Blanchard, and K. Tanaka, "Single-cycle terahertz pulses with amplitudes exceeding $1MV/cm$ generated by optical rectification in $LiNbO_3$," Appl. Phys. Lett. **98**, art. No. 091106 (2011).

[14] M. Kunitski, M. Richter, M. D. Thomson, A. Vredenborg, J. Wu, T. Jahnke, M. Schöffler, H. Schmidt-Böcking, H. G. Roskos, and R. Dörner, "Optimization of single-cycle terahertz generation in $LiNbO_3$ for sub-50 femtosecond pump pulses," Optics Express **21**, 6826–6836 (2013).

[15] H. Vincenti and F. Quéré, "Attosecond lighthouses: How to use spatiotemporally coupled light fields to generate isolated attosecond pulses," Phys. Rev. Lett. **108**, art. No. 113904 (2012).

[16] J. A. Fülöp and J. Hebling, "Applications of tilted-pulse-front excitation," in Recent Optical and Photonic Technologies, Ed. Ki Young Kim, ISBN 978-953-7619-71-8, 207–230 (2010).

[17] G. Pretzler, A. Kasper, and K. J. Witte, "Angular chirp and tilted light pulses in CPA lasers," Appl. Phys. B **70**, 1–9 (2000).

[18] K. Osvay, A. P. Kovacs, Z. Heiner, G. Kurdi, J. Klebniczki, and M. Csatari, "Angular dispersion and temporal change of femtosecond pulses from misaligned pulse compressors," IEEE J. Quant. Electron. **10**, pp.213–220 (2004).

[19] P. Bowlan, P. Gabolde, A. Shreenath, K. McGresham, R. Trebino, and S. Akturk, "Crossed-beam spectral interferometry: a simple, high-spectral-resolution method for completely characterizing complex ultrashort pulses in real time," Optics Express **14**, 11892–11900 (2006).

[20] M. R. Topp and G. C. Orner, "Group dispersion effects in picosecond spectroscopy," Opt. Commun. **13**, 276–281 (1975).

[21] N. H. Schiller and R. R. Alfano, "Picosecond characteristics of a spectrograph measured by a streak camera/video readout system," Opt. Commun. **35**, 451–454 (1980).

[22] O. Martinez, "Pulse distortions in tilted pulse schemes for ultrashort pulses," Opt. Commun. **59**, 229–232 (1986).

[23] C. Fiorini, C. Sauteret, C. Rouyer, N. Blanchot, S. Seznec, and A. Migus, "Temporal aberrations due to misalignments of a stretcher-compressor system and compensation," IEEE J. Quant. Electron. **QE-30**, 1662–1670 (1994).

[24] A. Kasper, G. Pretzler, and K. Witte, "100 or 300fs? Unnoticed pulse lengthening in the focus resulting from a tilted pulse front at the exit of a CPA-laser system," Verh. der DPG (VI) **33**, 223 (1998).

[25] C. Radzewicz, M. J. la Crone, and J. Krasinski, "Interferometric measurement of femtosecond pulse distortion by lenses," Opt. Commun. **126**, 185–190 (1996).

[26] S. Ameer-Beg, A. Langley, I. Ross, W. Shaikh, and P. Taday, "An achromatic lens for focusing femtosecond pulses: Direct measurement of femtosecond pulse front distortion using second-order autocorrelation technique," Opt. Commun. **122**, 99–104 (1996).

[27] C. Radzewicz, J. S. Krasinski, M. J. la Crone, M. Trippenbach, and Y. B. Band, "Interferometric measurement of femtosecond wave-packet tilting in rutile crystal," J. Opt. Soc. Am. B **14**, 420–424 (1997).

[28] A. A. Maznev, T. F. Crimmins, and K. A. Nelson, "How to make femtosecond pulses overlap," Opt. Lett. **23**, 1378–1380 (1998).

[29] Z. Sacks, G. Mourou, and R. Danielius, "Adjusting pulse-front tilt and pulse duration by use of a single-shot autocorrelator," Opt. Lett. **26**, 462–464 (2001).

[30] G. Figueira, L. Cardoso, N. Lopes, and J. Wemans, "Mirrorless tilted pulse front single-shot autocorrelator," J. Opt. Soc. Am. B **22**, 2709–2714 (2005).

[31] A. K. Sharma, R. K. Patidar, M. Raghuramaiah, P. A. Naik, and P. D. Gupta, "Measuring pulse-front tilt in ultrashort pulse laser beams without ambiguity of its sign using single-shot tilted pulse front autocorrelator," Optics Express **22**, 13131–13141 (2006).

[32] K. Varjú, A. P. Kovács, G. Kurdi, and K. Osvay, "High-precision measurement of angular dispersion in a CPA laser," Appl. Phys. B **74**, S259–S263 (2002).

[33] S. Arkturk, M. Kimmel, P. O'Shea, and R. Trebino, "Measuring pulse-front tilt in ultrashort pulses using GRENOUILLE," Optics Express **11**, 491–501 (2003).

[34] T. C. Wong and R. Trebino, "Single-frame measurement of complex laser pulses tens of picoseconds long using pulse-front tilt in cross-correlation frequency-resolved optical gating," J. Opt. Soc. Am. B **30**, 2781–2786 (2013).

[35] W. Amir, T. A. Planchon, C. G. Durfee, J. A. Squier, P. Gabolde, R. Trebino, and M. Müller, "Simultaneous visualization of spatial and chromatic aberrations by two-dimensional Fourier transform spectral interferometry," Opt. Lett. **31**, 2927–2929 (2006).

[36] W. Amir, T. A. Planchon, C. G. Durfee, and J. A. Squier, "Complete characterization of a spatiotemporal pulse shaper with two-dimensional Fourier transform spectral interferometry," Opt. Lett. **32**, 939–941 (2007).

[37] A. Börzsönyi, L. Mangin-Thro, G. Cheriaux, and K. Osvay, "Two-dimensional single-shot measurement of angular dispersion for compressor alignment," Opt. Lett. **38**, 410–412 (2013).

[38] M. Divoky and P. Straka, "Simple two-dimensional-imaging spectrograph with wedged narrow band filters," Rev. Sci. Instrum. **79**, art. No. 123114 (2008).

[39] M. Hornung, R. Bödefeld, M. Siebold, M. Schnepp, J. Hein, R. Sauerbrey, and M. C. Kaluza, "Alignment of a tiled-grating compressor in a high-power chirped-pulse amplification laser system," Appl. Opt. **46**, 7432–7435 (2007).

[40] F. Grasbon, A. Dreischuh, G. G. Paulus, F. Zacher, and H. Walther, "Femtosecond interferometric autocorrelations in the presence of pulse front distortions," Proc. SPIE **3571**, 164–168 (1999).

[41] D. Kreier and P. Baum, "Avoiding temporal distortions in tilted pulses," Opt. Lett. **37**, 2373–2375 (2012).

[42] R. Banici, R. Dabu, and D. Ursescu, "Characterization of tilted ultrashort pulses using a second harmonic inverted field autocorrelator," Internat. Conf. "Light at Extreme Intensities" (Oct. 16-21, 2009, Brasov, Romania) P11.

[43] N. Gorunski, N. Dimitrov, A. Dreischuh, and G. G. Paulus, "Pulse-front tilt created in misaligned dispersionless optical systems and correct interferometric autocorrelation," Opt. Commun. **283**, 5192–5198 (2010).

[44] Z. L. Horvath, Z. Benko, A. P. Kovacs, H. A. Hazim, and Z. Bor, "Propagation of femtosecond pulses through lenses, gratings, and slits," Opt. Eng. **32**, 2491–2500 (1993).

[45] K. Varjú, A. P. Kovács, K. Osvay, and G. Kurdi, "Angular dispersion of femtosecond pulses in a Gaussian beam," Opt. Lett. **27**, 2034–2036 (2002).

[46] N. Dimitrov, L. Stoyanov, I. Stefanov, A. Dreischuh, P. Hansinger, and G. G. Paulus, "Measuring the relation between pulse-front-tilt angle and beam size for ultrashort laser pulses," Bulg. J. Phys. **43**, 21–29 (2016).